Supporting Information

Kinetic Study of Hydrogen Evolution Reaction over Strained MoS$_2$ with Sulfur Vacancies Using Scanning Electrochemical Microscopy

Hong Li[1†], Minshu Du[2†], Michal J. Mleczko[3], Ai Leen Koh[4], Yoshio Nishi[3], Eric Pop[3,5], Allen J. Bard[2]★ and Xiaolin Zheng[1]★

[1]Department of Mechanical Engineering, Stanford University, Stanford, California 94305, United States

[2]Center for Electrochemistry, Department of Chemistry, The University of Texas at Austin, Austin, Texas 78712, United States

[3]Department of Electrical Engineering, Stanford University, Stanford, California 94305, United States

[4]Stanford Nano Shared Facilities, Stanford University, Stanford, California 94305, United States

[5]Precourt Institute for Energy, Stanford University, Stanford California 94305, United States

e-mail: Allen J. Bard: ajbard@cm.utexas.edu, Xiaolin Zheng: xlzheng@stanford.edu

[†]These authors contributed equally to this work.

Supporting Figures
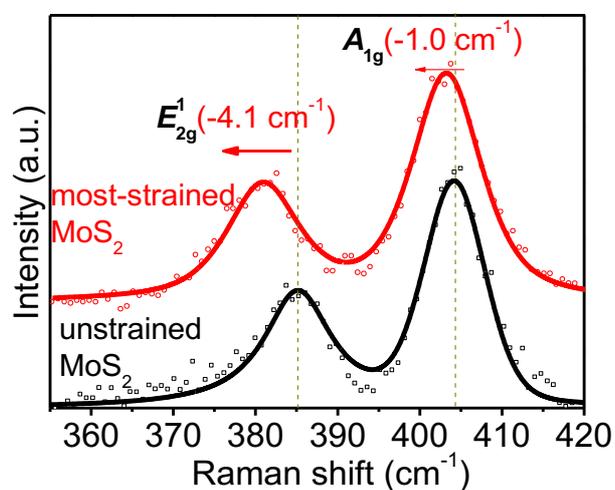
Figure S1. Raman spectrum of unstrained and most-strained (on top of nanopillar) monolayer MoS_2. The open symbols and solid lines represent the measured and fitting data, respectively. Vertical dashed lines indicate the positions of E^1_{2g} and A_{1g} peaks of unstrained MoS_2. From the magnitude of redshifts (arrows) of Raman peaks, the magnitude of the uniaxial tensile strain is estimated to be ~ 2%.
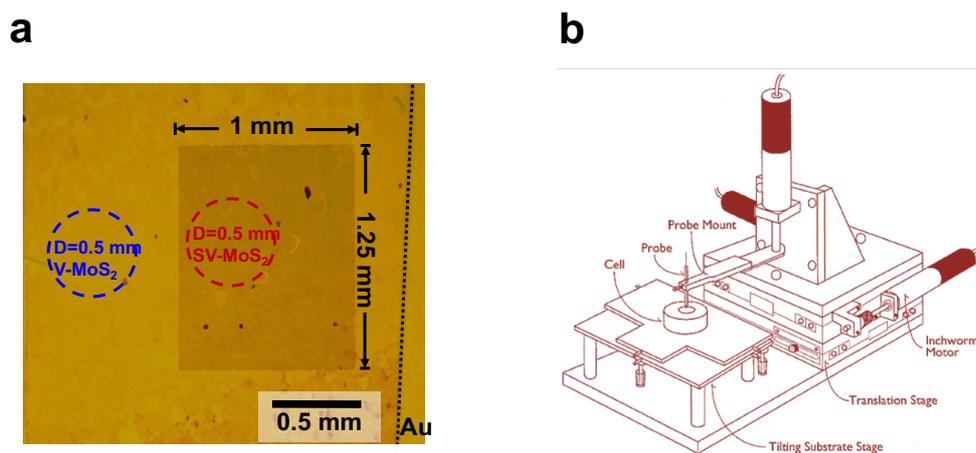
Figure S2. Scanning electrochemical microscopy characterization of the HER kinetics of MoS_2. (a) a 0.5 mm diameter V-MoS_2 electrode and a 0.5 mm diameter SV-MoS_2 electrode were fabricated next to each other on the same substrate. The rest exposed surface areas are covered by plastic tape in order to be clear of the electrolyte. The 1 mm by 1.25 mm rectangle part corresponds to SV-MoS_2, which has a monolayer MoS_2 on top of gold nanopillars. (b) Schematic illustration of translators, tip and cell mounts of the commercially available CH model 920C SECM (reproduced in page 43 from reference[1] with permission. Copyright 2001 by Marcel Dekker, Inc.). In our experiment, the probe was a 25 μm diameter Pt UME, and the substrate was a 0.5 mm diameter MoS_2 electrode, and another Pt wire and Ag/AgCl electrode were used as the counter and reference electrodes, respectively, fixed in the cell. The electrolyte was the Ar-saturated 0.1 M $HClO_4$ solution.

a

simulation parameters:
$E^0 = -0.4$ V
$K_{tip}^0 = 10$ cm/s
Alpha = 0.5
$E_{tip} = -0.35$ V
$K_{sub} = 0$ cm/s
c = 0.1 M
tip/substrate distance is ~ 5 μm

• Experiment
○ Simulation

y-axis: I / I_∞
x-axis: d / a

b

simulation parameters:
$E^0 = -0.4$ V
$K_{tip}^0 = 10$ cm/s
Alpha = 0.5
$E_{tip} = -0.35$ V
$K_{sub} = 0$ cm/s
c = 0.1 M
tip/substrate distance is ~ 4 μm

• Experiment
○ Simulation
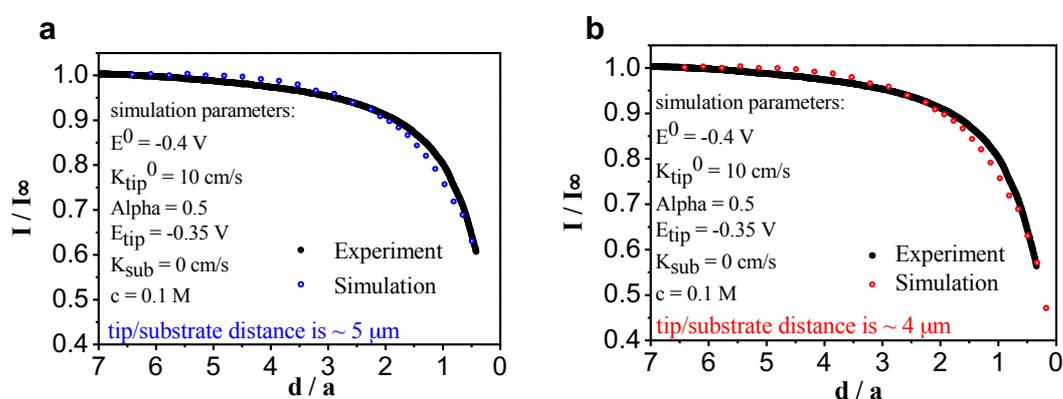
y-axis: I / I_∞
x-axis: d / a

Figure S3. Measured and calculated SECM approach curves upon V-MoS$_2$ (a) and SV-MoS$_2$ (b) substrates with tip potential at -0.35 V in 0.1 M HClO$_4$. The *y* axis is the normalized tip current I/I$_\infty$, where I$_\infty$ is the tip current when it is far from the substrate. The *x* axis is the normalized distance d/a, where d is the real tip-substrate distance and a is the radius of the tip.
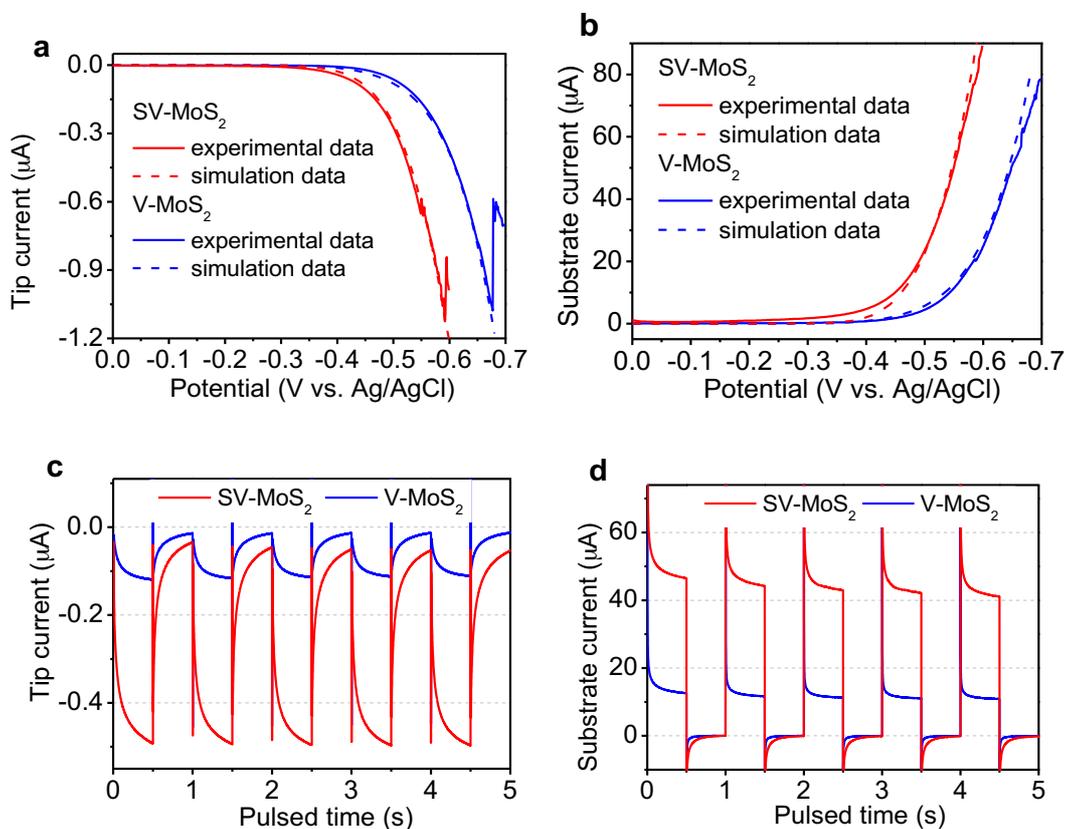
Figure S4. Comparison of the HER activities of V-MoS$_2$ and SV-MoS$_2$. (a) Pt tip and (b) substrate currents of V-MoS$_2$ and SV-MoS$_2$ substrates from LSV measurements in 0.1 M HClO$_4$ solution and the corresponding simulation results (dashed curves). Tip potential was held at 0 V, and the substrate potential was swept from 0 V to -0.7 V at a scan rate of 5 mV/s. Transient (c) Pt tip and (d) substrate currents according to the double-pulse potential applied to the substrate. Tip potential was held at 0 V, and the substrate potential was switched between open circuit potential and -0.55 V (vs. Ag/AgCl) to enable MoS$_2$ for the HER. The pulse width was 0.5 s with 5 replicates.
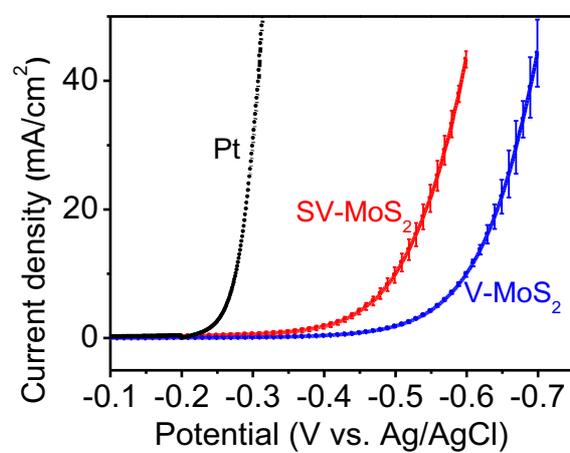
Figure S5. Polarization curves of MoS$_2$ with S vacancies. LSV curves of V-MoS$_2$ and SV-MoS$_2$ electrodes on the same substrate in 0.1 M HClO$_4$ solution at a scan rate of 50 mV/s. The error bars represent the standard deviation from four repeated measurements. For comparison, the Pt LSV curve was obtained on 25 μm diameter Pt UME after activation.
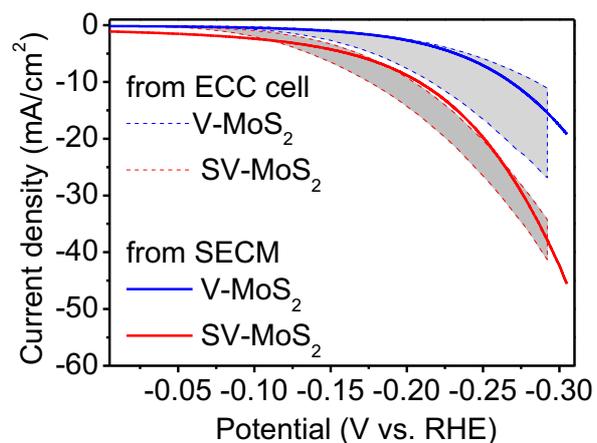
Figure S6. Complementary LSV measurements. LSV curves of V-MoS$_2$ and SV-MoS$_2$ using a three-electrode electrochemical compression (ECC) cell (3 mm in diameter) compared to those obtained with Pt UME tip (0.5 mm in diameter) in SECM. The shaded areas represent the range of LSV curves from 8 samples measured in 0.3 M H$_2$SO$_4$ using ECC cell. There is a good agreement between ECC and SECM measurements.
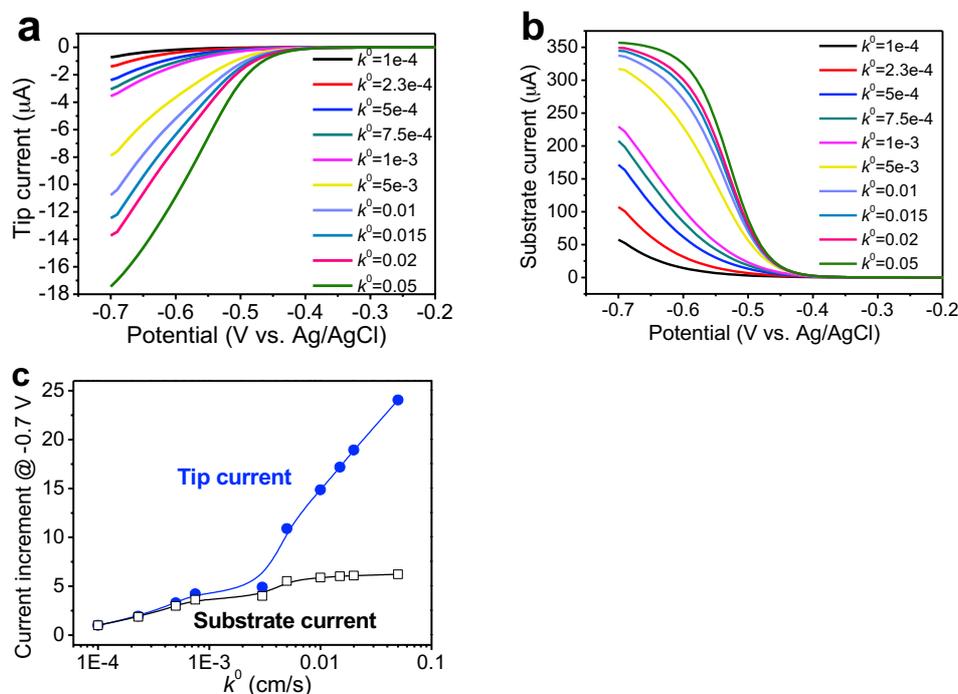
Figure S7. Simulated LSV plots of (a) Pt tip electrode and (b) MoS$_2$ substrate electrode in the SG-TC mode of the SECM with various kinetic rate constants k^0 for the HER on the MoS$_2$ substrate in a 0.1 M acidic electrolyte. Multiphysics simulation was performed using COMSOL Multiphysics software. The simulated parameters include: HOR kinetic parameters on a 12.5 μm radius Pt UME (E_t^0 = -0.40 V, α_t = 0.5, k_t^0 = 0.42 cm/s), HER kinetic parameters on a 250 μm radius MoS$_2$ electrode (E_s^0 = -0.53 V, α_s = 0.4, k_s^0 as annotated in the figure), and the tip-substrate distance of 4 μm. In the simulation, tip potential was held at 0 V and the substrate potential was swept from -0.2 V to -0.7 V at a scan rate of 5 mV/s. (c) Normalized current increment (by the current of k^0 = 1e-4) at various k^0 values at potential of -0.7 V for both tip (solid symbols) and substrate current (open symbols).

Supporting Note 1

Sample fabrication

The sample fabrication started with a polished SiO_2/Si wafer. Electron-beam lithography was used to pattern dotted arrays with electron-beam resist, which served as the etching mask. Dry etching (a mixture of CHF_3 and O_2 gases) was used to etch away 80 nm thick SiO_2. As a result, a SiO_2 nanopillar array was created in the center of the wafer after removal of resist. The pitch size is 650 nm, and the diameter and height of the nanopillars are 350 nm and 80 nm, respectively. A gold (90 nm)/titanium (10 nm) bilayer film was deposited onto the wafer to metallize the substrate. Quasi-continuous $2H$-MoS_2 monolayers were grown on SiO_2 substrate in a homemade tube furnace.[2] PMMA was spun coated onto the as-grown sample containing MoS_2 monolayers. The sample was etched in 1M KOH solution at 80 ^{o}C for a couple hours so that the PMMA/MoS_2 bilayer film was lift off and floated on the surface of the KOH solution. Then the PMMA/MoS_2 film was transferred into DI water to remove the KOH residue. This process was repeated a few times to completely remove KOH residue on the film. Afterward, the patterned substrate was used to scoop the PMMA/MoS_2 film so that it covered both flat area and the nanopillar array. Then the sample was baked at 100 ^{o}C for 10 minutes to dry the water and increase the adhesion between MoS_2 and substrate. In order to completely remove the PMMA, the sample was successively soaked in acetone and chloroform at 60 ^{o}C for 10 and 60 minutes, respectively. The sample was then soaked in ethylene glycol in vacuum for one hour, followed by completely evaporation of ethylene glycol. The capillary force in ethylene glycol drying process generates elastic strains in MoS_2.[3] In order to generate S vacancies, the transferred MoS_2 samples were exposed to a cold and mild argon plasma that was generated by 4 W rf power in a 6 inch diameter chamber at 1 bar. A well-controlled desulfurization process was performed to generate S vacancies (see our previous work for more details[2]). Finally, SV-MoS_2 was obtained in the nanopillar area while V-MoS_2 was obtained in the flat area not covered by nanopillars.

Sample characterization

Raman spectroscopy was used to obtain quantitative information of elastic strain in the sample that has a well-established relation with Raman shift.[3,4] Raman modes (in-plane E_{2g}^1 and out-of-plane A_{1g}) of monolayer MoS_2 show red shifts upon tensile strain. The red shift ratio of E_{2g}^1 and A_{1g} modes are 2.2 cm^{-1}/% and 0.5 cm^{-1}/%, respectively, for uniaxial tensile strain.[3,4] The amount of S vacancy was quantified using a transmission electron microscope [FEI spherical aberration (image)-corrected 80-300 Titan environmental (scanning) (FEI Titan E-(S)TEM) operated at 80 kV] and negative Cs imaging technique, and is consistent with X-ray photoelectron spectroscopy measurement, as shown in our earlier work.[2]

Supporting Note 2

Substrate electrode preparation

The 0.5 mm diameter MoS_2 working electrodes were defined by masking the prepared MoS_2 substrate using a plastic tape with two hole openings. The holes in the tape were punched by a Harris Micro-Punch[®] with a 0.5 mm diameter needle (Ted Pella Inc, Redding, CA). One hole was located on the unstrained MoS_2 area (V-MoS_2) and the other was on the nearby strained MoS_2 area, *i.e.*, the gold nanopillar array (SV-MoS_2). Only the MoS_2 within these two holes were exposed to the electrolyte. As such, the 0.5 mm diameter V-MoS_2 and SV-MoS_2 working electrodes were obtained, as illustrated in Figure S2a.

Pt UME tip preparation

A 2 cm long and 25 μm thick Pt wire (Alfa Aesar, 99.95% purity, Ward Hill, MA) was sealed into a borosilicate capillary with 1.5 mm outer diameter and 0.75 mm inner diameter (FHC, Bowdoin, ME) under vacuum. One end of the borosilicate capillary was polished with 600 mesh sandpaper (Buehler, Lake Bluff, IL) until the metal disk was exposed and then sharpened and smoothed with a 3 μm diamond lapping film and another 0.1 μm diamond lapping film (Allied, Rancho Dominguez, CA) successively. The ratio of glass to metal radius (RG) of the tip was about 2. Silver-epoxy (Epo-tek H20E, Epoxy Technology, Billerica, MA) cured overnight at 100 ºC was used to make electric contact between the Pt wire and a 0.143 mm diameter NiCr wire (Alfa Aesar, Ward Hill, MA).

Electrochemical measurements

A 920C SECM (CH Instruments, Austin, TX) setup was employed, as shown schematically in Figure S2b. The MoS_2 substrate was placed between an acrylic base and a PTFE cell with a 3.8 mm diameter orifice in the center. An O-ring with a 1.8

mm inner diameter was used to ensure a leakage-free connection. A 25 μm diameter Pt UME served as the tip which was mounted facing the substrate electrode downwards. A Pt wire was used as a counter electrode, and a Ag/AgCl (1M) electrode (CH Instruments, Austin, TX) served as a reference electrode. All the potentials showed in this paper were relative to Ag/AgCl (1M) reference electrode unless stated otherwise. For the SECM experiments, a sealed glove bag was purged with Ar to remove oxygen. All the SECM measurements were performed in 0.1 M HClO$_4$ aqueous solution after deaeration (Ar bubbling).

The 0.5 mm diameter V-MoS$_2$ and SV-MoS$_2$ working electrodes were studied successively by being individually placed within the O-ring area. The measurement is schematically illustrated in Figure 1a. After approaching the tip to the substrate by the negative feedback of proton reduction on the Pt, hydrogen was electrogenerated from proton in the 0.1 M HClO$_4$ ($H^+ + e^- \rightarrow \frac{1}{2}H_2$) at the MoS$_2$ working electrode. Then hydrogen diffused away from the substrate, and parts of it was collected by the Pt UME tip held at 0 V where hydrogen underwent diffusion-controlled oxidation back into the proton ($\frac{1}{2}H_2 \rightarrow H^+ + e^-$). Two kinds of substrate generation-tip collection (SG-TC) modes were applied. Firstly, the MoS$_2$ substrate potential was swept from 0 V to -0.7 V at a scan rate of 5 mV/s to generate hydrogen continuously, and the hydrogen was then collected at the Pt UME tip. Secondly, the MoS$_2$ substrate potential was switched between the open circuit potential and the negative potentials for HER by dual-potential steps. The pulse width was 0.5 s with 5 replicates. Also, the tip potential was held at 0 V as an amperometric sensor for collecting and oxidizing the hydrogen molecules.

Moreover, in order to test the repeatability of the HER activities of V-MoS$_2$ and SV-MoS2 samples, a three-electrode electrochemical compression cell was used for electrochemical measurements on 8 samples with a Gamry 600 potentiostat. The MoS$_2$ sample served as the working electrode; A Pt wire acted as the counter electrode; and an Ag|AgCl electrode was used as the reference electrode. 0.3 M Sulfuric acid

(H_2SO_4) with pH value of 0.2 was used as the electrolyte.

Supporting Note 3

Multiphysics simulation

To compare the kinetic effects of strain, it is useful to have a model of the electron-transfer reaction. The HER of MoS_2 is complex, and no recognized model exists so far. We chose to investigate this by a simple n = 1 electron transfer with a Butler-Volmer formalism.[5]

For SECM SG-TC experiments, digital simulations were performed using COMSOL Multiphysics software v4.2 (COMSOL, Inc., Burlington, MA). Two-dimensional axial symmetry model was employed (see Figure 1b), a 12.5 μm radius Pt UME (a = 12.5 μm, RG = 2) and a 250 μm radius MoS_2 working electrode (b = 250 μm) vertically aligned in a cylinder with a radius of 500 μm and a height of 500 μm. The distance between the tip and substrate was 5 μm for V-MoS_2 and 4 μm for SV-MoS_2.

The concentration of H^+ (O) and H_2 (R) were determined throughout the geometry by solving Fick's Second Law of Diffusion in cylindrical coordinates for both species:

$$\frac{\partial C_o}{\partial t} = D_o \left[\frac{\partial^2 C_o}{\partial r^2} + \frac{1}{r}\frac{\partial C_o}{\partial r} + \frac{\partial^2 C_o}{\partial z^2} \right]$$

$$\frac{\partial C_R}{\partial t} = D_R \left[\frac{\partial^2 C_R}{\partial r^2} + \frac{1}{r}\frac{\partial C_R}{\partial r} + \frac{\partial^2 C_R}{\partial z^2} \right]$$

$$\tag{1}$$

where C is the concentration and D is the diffusion coefficient. The reported values of 7.9×10^{-5} cm^2/s for the diffusion coefficient of H^+ (D_O)[6] and 5×10^{-5} cm^2/s for the diffusion coefficient of H_2 (D_R)[7] were used.

The flux boundary conditions were set on the tip and substrate electrodes as shown in Equation 2:

$$J_{\text{tip}} = K_{\text{ft}} \cdot C_{\text{O}} - K_{\text{bt}} \cdot C_{\text{R}}$$

$$J_{\text{sub}} = -K_{\text{fs}} \cdot C_{\text{O}} + K_{\text{bs}} \cdot C_{\text{R}}$$

(2)

where K_{ft} and K_{bt} are the forward and backward rate constant, respectively, for Pt UME tip, and K_{fs} and K_{bs} are the forward and backward rate constant, respectively, for MoS$_2$ working electrode with:

$$K_{\text{ft}} = k_{\text{t}}^0 \cdot e^{[-\alpha_{\text{t}} \cdot n \cdot f \cdot (E_{\text{tip}} - E_{\text{t}}^0)]}$$

$$K_{\text{bt}} = k_{\text{t}}^0 \cdot e^{[(1 - \alpha_{\text{t}}) \cdot n \cdot f \cdot (E_{\text{tip}} - E_{\text{t}}^0)]}$$

$$K_{\text{fs}} = k_{\text{s}}^0 \cdot e^{[-\alpha_{\text{s}} \cdot n \cdot f \cdot (E_{\text{sub}} - E_{\text{s}}^0)]}$$

$$K_{\text{bs}} = k_{\text{s}}^0 \cdot e^{[(1 - \alpha_{\text{s}}) \cdot n \cdot f \cdot (E_{\text{sub}} - E_{\text{s}}^0)]}$$

(3)

where $f = F / RT$ and k_{t}^0, α_{t}, E_{t}^0 were assumed to be 0.42 cm/s, 0.5, -0.40 V, respectively.

Time-dependent H$^+$ and H$_2$ distributions were simulated and expressed by color-coded profile (see the concentration profile of H$_2$ when the SV-MoS$_2$ substrate potential was fixed at -0.6 V in main Figure 1b).

The currents on the tip and substrate were calculated using Fick's First Law of Diffusion:

$$\frac{i}{nFA} = -J(t) = D_{\text{O}} \frac{\partial C_{\text{O}}}{\partial z}$$

(4)

Where i is the current, n is the electron number, F is Faraday's constant, A is the electrode area, and J is the flux.

As the scan rate of the SG-TC experiment was sufficiently slow (5 mV/s), we used the steady-state solver to obtain the simulation for the potential sweep experiments. The kinetic parameters of HER for V-MoS$_2$ and SV-MoS$_2$ including the formal potential E^0, electro-transfer coefficient α_{s} and the rate constants k^0 were determined by finding the best fit between experimental and simulated linear sweep

voltammograms for both the tip and the substrate.

Since a 0.5 mm diameter MoS_2 substrate has a much larger ohmic drop compared to that of a 25 μm diameter Pt tip, the best fit simulated HOR LSV curve on the Pt tip was firstly obtained by the least square method, which was controlled by a set of HER kinetic parameters on the MoS_2. Then, the obtained set of parameters were used to simulate the HER LSV curve on the MoS_2 substrate and compared to the corresponding experimental LSV curve.

Figures S7a and S7b show the simulated LSV curves at various kinetic rate constant k^0 for both tip and substrate current, respectively. Figure S7c summarizes the normalized current increment (normalized to that of $k^0 = 1e-4$) at -0.7 V. The current change is much more obvious on the tip electrode in the SG-TC SECM mode compared to that of the much larger MoS_2 electrode when k^0 varies in the same range. Therefore, SG-TC mode of the SECM has a higher degree of sensitivity and accuracy for studying the reaction kinetics.

Supporting References

1. Bard, A. J.; Faulkner, L. R. *Electrochemical methods: fundamentals and applications*. Vol. 2 (Wiley New York, 1980).
2. Li, H.; Tsai, C.; Koh, A. L.; Cai, L.; Contryman, A. W.; Fragapane, A. H.; Zhao, J.; Han, H. S.; Manoharan, H. C.; Abild-Pedersen, F.; Nørskov, J. K.; Zheng, X. *Nat. Mater.* **2016**, *15*, 48-53.
3. Li, H.; Contryman, A. W.; Qian, X.; Ardakani, S. M.; Gong, Y.; Wang, X.; Weisse, J. M.; Lee, C. H.; Zhao, J.; Ajayan, P. M.; Li, J.; Manoharan, H. C.; Zheng, X. *Nat. Commun.* **2015**, *6*, 7381.
4. Rice, C.; Young, R. J.; Zan, R.; Bangert, U.; Wolverson, D.; Georgiou, T.; Jalil, R.; Novoselov, K. S. *Phys. Rev. B* **2013**, *87*, 081307.
5. Du, M.; Cui, L.; Cao, Y.; Bard, A. J. *J. Am. Chem. Soc.* **2015**, *137*, 7397-7403.
6. Leonard, K. C.; Bard, A. J. *J. Am. Chem. Soc.* **2013**, *135*, 15890-15896.
7. Macpherson, J. V.; Unwin, P. R. *Anal. Chem.* **1997**, *69*, 2063-2069.